CHEMICAL ENGINEERING TRANSACTIONS
VOL. 27, 2012
A publication of AIDIC
The Italian Association of Chemical Engineering
Online at: www.aidic.it/cet
Guest Editors: Enrico Bardone, Alberto Brucato, Tajalli Keshavarz

ISBN 978-88-95608-18-1; **ISSN** 1974-9791
DOI: 10.3303/CET1227035

Oxygen Transfer Performance of Unbaffled Stirred Vessels in View of Their Use as Biochemical Reactors for Animal Cell Growth

Francesca Scargiali, Antonio Busciglio, Franco Grisafi and Alberto Brucato

Dipartimento di Ingegneria Chimica, Gestionale, Informatica e Meccanica, Università degli Studi di Palermo, Viale delle Scienze, Ed. 6, 90128, Palermo, Italy
francesca.scargiali@unipa.it

Cultivation of microorganisms, plants or animal cells requires liquid agitation in order to ensure oxygen and nutrient transfer and to maintain cell suspension. However, in such suspensions both mechanical agitation and sparging aeration can cause cell death. Many studies on animal cell damage due to mechanical agitation and sparging aeration have shown that mechanical damage of freely suspended animal cells is in most cases associated with bursting bubbles at the air–liquid interface (Barrett et al., 2010; Nienow et al., 1996). Gas bubbles are usually generated by direct air sparging to propagate oxygen in a culture suspension. Mechanical agitation may also introduce gas bubbles to the culture fluid through vortexing entrainment from the free surface. In this work oxygen transfer performance of an unbaffled stirred vessel is presented in view of its use as biochemical reactor for animal cell growth. As a matter of fact, oxygen mass transfer can occur through the free surface deep vortex which takes place when agitation is started. If this is not allowed to reach impeller blades, bubble formation and subsequent bursting inside the reactor is avoided. Experimental results showed that this kind of bioreactor may well provide sufficient oxygen mass transfer for animal cell growth so resulting in a valid alternative to more common sparged reactors. Clearly this potential needs to be confirmed by *in vivo* experimentation, before firm conclusions are drawn.

1. Experimental

The experimental apparatus is depicted in Figure 1. It involved a PMMA made cylindrical stirred reactor (D_T = 190 mm) with a total height of 300 mm. A “Rushton turbine” (six flat blade disk mounted) of 65 mm dia. was mounted on the 17 mm dia. shaft, leaving a clearance of T/3 from vessel bottom. The vessel was filled with deionized water up to an eight of 190 mm (H=T) under no agitation conditions.
A static frictionless turntable and a precision scale were employed for measuring the mechanical power dissipated by the impeller at various agitation speeds and gas flow rates. Details of this apparatus are given by Grisafi et al. (1998).
The volumetric mass transfer coefficient, k_La, was assessed by unsteady state experiments by means of the simplified dynamic pressure method (SDPM) (Scargiali et al., 2010 a and b). In this method the driving force for oxygen absorption is obtained by a sudden change of vessel pressure, with no need for sudden gas phase composition changes. In particular, pressure inside the reactor was typically brought down to about 0.5 bar while stirring at high agitation speeds to fasten the degassing process. Pressure and agitation were maintained for a time (1 – 2 min) sufficient to allow for dissolved oxygen and nitrogen concentrations in the liquid phase to go down towards equilibrium with air at 0.5 bar.

Please cite this article as: Scargiali F., Busciglio A., Grisafi F. and Brucato A., 2012, Oxygen transfer performance of unbaffled stirred vessels in view of their use as biochemical reactors for animal cell growth, Chemical Engineering Transactions, 27, 205-210
DOI: 10.3303/CET1227035

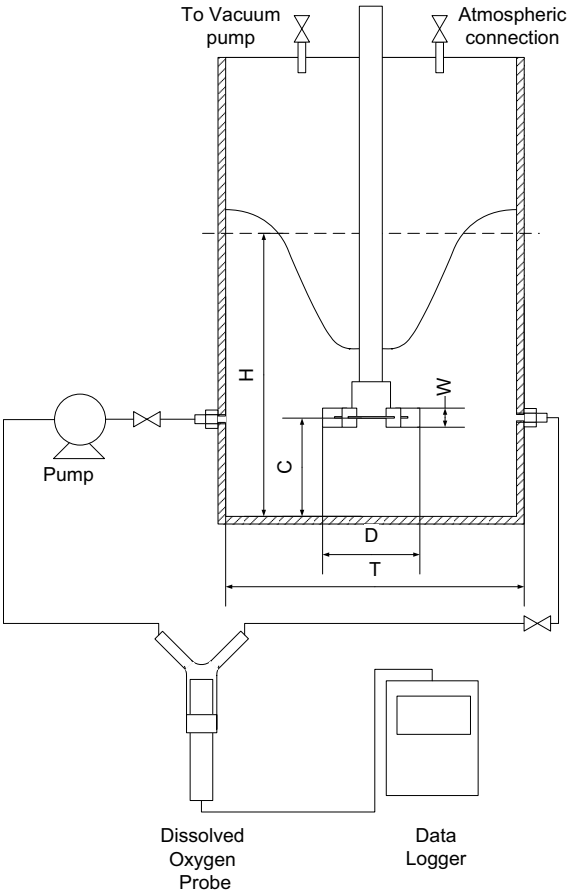

Figure1: Schematic diagram of the experimental apparatus

Agitation speed was then adjusted to the required value and after regime conditions were attained atmospheric pressure was suddenly restored, by simply admitting air to the reactor headspace through a suitable valve. A transitory followed, in which the difference between equilibrium concentrations of both oxygen and nitrogen to air at 1 bar and the time dependent oxygen and nitrogen concentrations in the liquid phase decayed and eventually vanished. The dissolved-Oxygen concentration dynamics was measured via a suitable probe and the relevant time series was acquired by a PC. At the end of the transitory the stationary dissolved Oxygen concentration of about 9.3 ppm wt was reached inside the reactor.
The reactor was equipped by a stainless steel top to allow reactor evacuation. Oxygen concentration was measured by means of an electrode sensor (WTW CellOx 325) and control unit (WTW Oxi 340i). The electrode time constant was experimentally measured to be about 3.0 s thus a value significantly smaller than the expected time dynamics for oxygen absorption, so that neglecting the probe time dynamics certainly has negligible effects on the resulting k_La values (Van't Riet, 1979; Scargiali et al, 2010). Rotational speed ranged from 100 to 1300 rpm in order to explore different fluid-dynamics regimes occurring inside the unbaffled stirred reactor.

2. Results and discussion

2.1 Power consumption

The specific power dissipation values obtained at the various agitation speeds by the static frictionless turntable are reported in Figure 2a.

A steep increase of power dissipation with agitation speed is observed, as expected. In the same figure the agitation speed at which the free surface vortex reaches the impeller is marked by an empty symbol. The relevant total power dissipation was translated into power number (N_p) values, defined as

$$N_p = \frac{P}{\rho_L N^3 D^5} \quad (1)$$

where P is agitation power, ρ_L is liquid density, N is agitation speed (s^{-1}) and D is impeller diameter.

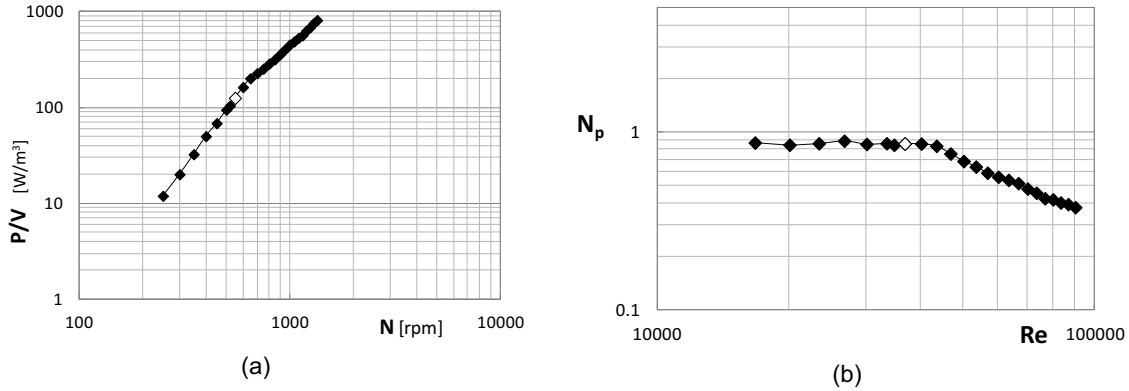

Figure 2: Experimental specific power dissipation (a) and relevant Power Number (b). The empty symbol marks the critical rotational speed (N_{crit}) (a) and Reynolds Number (b) at which the free surface vortex reaches the impeller

Power Number results are reported in Figure 2b, where it can be observed that power number is almost constant until the free surface vortex reaches the impeller to subsequently decrease. As a matter of fact, at higher agitation speeds air begins to be dispersed inside the reactor and vortex cavities appear behind the blades strongly reducing power consumption as typically occurs in sparged reactors (Middleton, 1985).

2.2 k_La measurements

A typical oxygen concentration dynamics in the liquid phase, obtained at 650 rpm, is shown in Figure 3, where the dimensionless driving force for mass transfer is plotted versus time on a semi-log diagram. As it can be seen, the model prediction that curve slope should eventually settle over a straight line is fully confirmed . The final slope observed of -0.00478 s^{-1} practically coincides with $-k_La$ as for values lower than 0.05 s^{-1} no slope correction is needed (Scargiali et al., 2010a,b).

The k_La values obtained in all other runs are reported in Figure 4 as a function of rotational speed. In the same figure an empty symbol marks the critical agitation speed. As it is possible to see the mass transfer coefficient increases as rotational speed increases, showing three different regions corresponding to different fluid dynamics regimes.

In particular, at the lowest rotational speeds, below 300 rpm, the liquid free surface is almost flat, no gas dispersion is present in the liquid phase and gas-liquid mass transfer occurs only through the flat surface. In this range the k_La varies only due to k_L increase, being the inter-phase surface area almost constant. Notably k_La is found to increase with a power law with exponent slightly larger than 0.5, the expected result on the basis of penetration theory when interfacial area is almost constant.

At rotational speeds higher than 300 rpm the free surface vortex becomes progressively more pronounced up to reaching the impeller at a rotational speed of about 550 rpm. In this range, no gas dispersion is present inside the reactor while interfacial area significantly increases due to vortex formation, making k_La versus N slope of the order of 5, as can be observed in Figure 4. This is a steeper dependence than expected on the basis of vortex shape change, possible related to the fact that vortex surface is not smooth, but rather rippling. At rotational speeds higher than 550 rpm air begins to be ingested in the liquid phase and an increasing gas dispersion is observed, somewhat

counterbalancing the lack of further increase of central vortex interfacial area. As a consequence k_La continues to increase with an exponent of about 3, smaller than 5 but still significantly larger than 0.5.
It is worth noting that in order to avoid gas dispersion inside the reactor, so preserving animal cell from bubble burst damage, an operating agitation speed smaller than the critical one (N_{crit}) should be used. In the present system this implies a maximum k_La value of about $1.3 \cdot 10^{-3}$ s^{-1}, as highlighted by the dotted line in Figure 4.

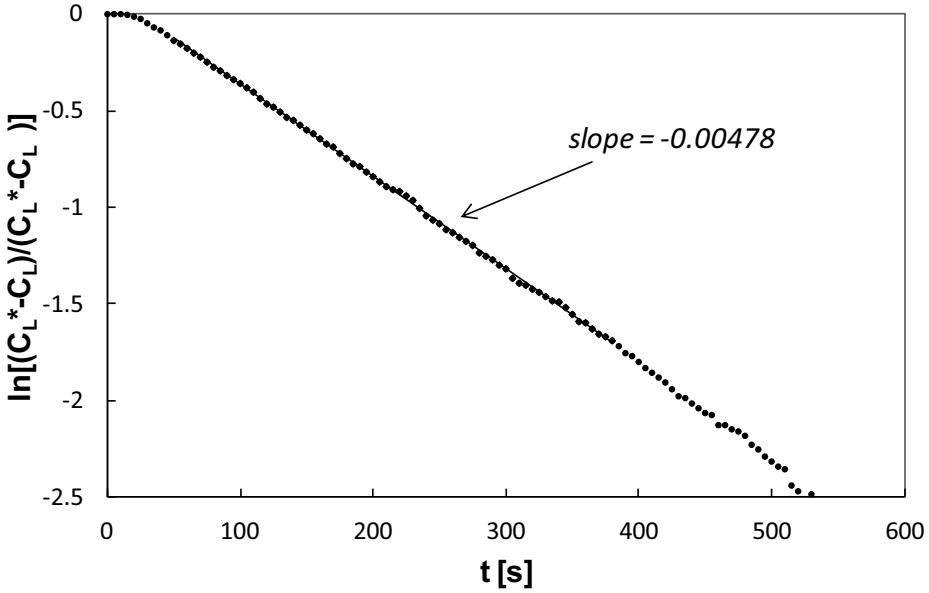

Figure 3: Typical oxygen concentration dynamics at N = 650 rpm

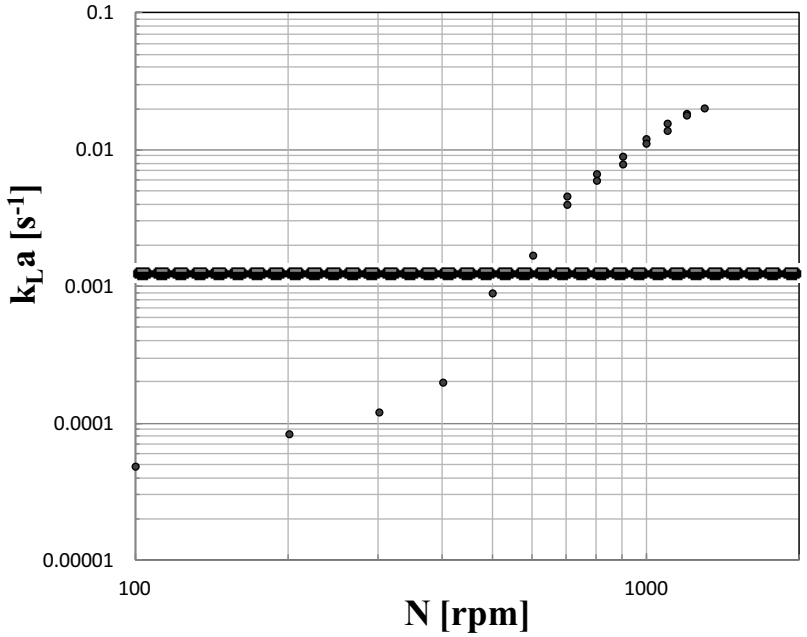

Figure 4: Experimental mass transfer coefficient vs rotational speed. The empty symbol represents the critical rotational speed (N_{crit}) and relevant mass transfer coefficient at which the free surface vortex reaches the impeller

Considering that mean specific oxygen up-take rates, q_{O2}, as measured in commercial respirometers, vary between 10^{-17} and 10^{-16} mol O_2/cell s (Nienow et al., 1996), and assuming a liquid phase oxygen concentration driving force of $1.3 \cdot 10^{-7}$ mol O_2/ml (50 % of saturation with ambient air) the oxygen up-take rate can be computed as:

$$W_{O_2} = k_L a \left(C_L^* - C_L\right) = 1.3 \cdot 10^{-3} \cdot 1.3 \cdot 10^{-7} = 1.7 \cdot 10^{-10} \text{ mol } O_2\text{/ml s} \quad (2)$$

which will support a maximum cell concentration $C_{cell} = \frac{W_{O_2}}{q_{O_2}}$ in the range of $1.7 \cdot 10^6$ and $1.7 \cdot 10^7$ cell/ml, hence values well consistent with animal cell bioreactor practice (Nienow et al., 1996). It can be concluded that unbaffled stirred vessels, with oxygen uptake only from the central vortex surface (no gas bubbles burst), can provide sufficient oxygen mass transfer for animal cell growth.

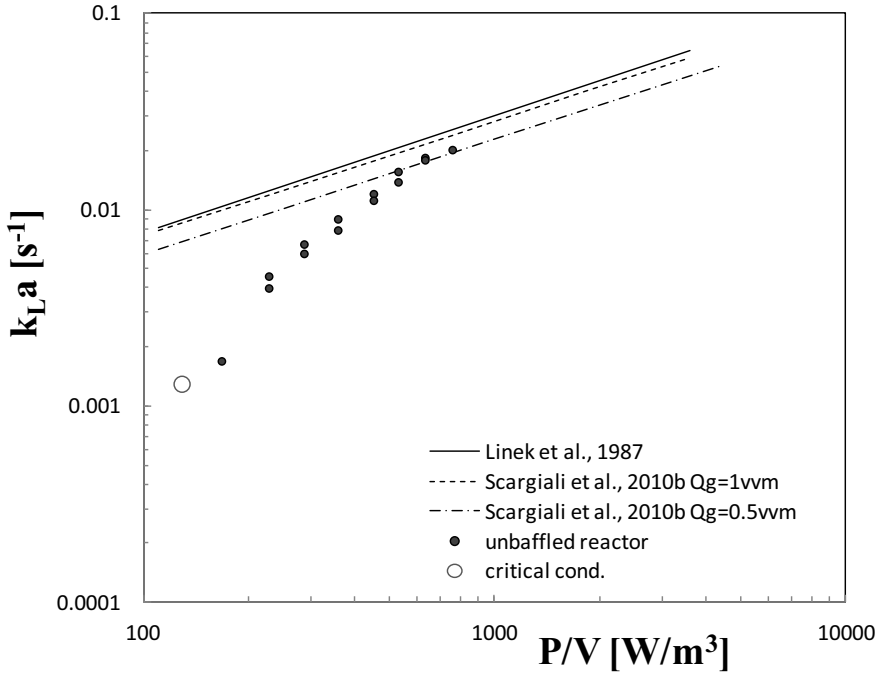

Figure 5: Comparison between mass transfer coefficients obtained in the unbaffled reactor and in standard gas-liquid sparged reactors

2.3 Comparison with other gas-liquid reactors

In Figure 5 the same data of Figure 4 are reported versus *specific power input*, in order to compare them on a suitable basis with literature data for standard *baffled sparged* stirred reactors, for different gas flow rates, depicted as straight lines on the basis of correlations proposed by Scargiali et al. (2010a,b) and by Linek et al. (1987). As in previous figures, the critical impeller speed is marked by an empty symbol.

As it is possible to observe the mass transfer performance of the unbaffled reactor is always poorer than in sparged baffled tanks, and becomes comparable with standard gas-liquid reactors only at specific power inputs larger than 500 W/m^3, when critical conditions have been widely overcome and gas entrapment and dispersion is occurring.

Nevertheless, as already noticed out, mass transfer coefficients of the order of 10^{-2} s^{-1} are not necessary to sustain the bioreactor cell concentrations commonly encountered in animal and plant cell

cultures, hence there is no point in incurring in cell damage due to bubble bursting in order to uselessly increase an already satisfactory mass transfer rate.

3. Conclusions

Oxygen transfer performance of an unbaffled stirred vessel has been presented in view of its use as biochemical reactor for animal cell growth. As a matter of fact, oxygen mass transfer can conveniently occur through the quite wide free vortex surface which forms when agitation is large enough, yet still insufficient to inject bubbles in the liquid, so bubble subsequent bursting and related cell damage is avoided.

Experimental results showed that this kind of bioreactor may well provide sufficient oxygen mass transfer for animal cell growth so resulting in a valid alternative to more common sparged reactors. Clearly this potential needs to be confirmed by *in vivo* experimentation, before firm conclusions are drawn.

References

Grisafi F., Brucato A., Rizzuti L., 1998, Solid–liquid mass transfer coefficients in gas–solid–liquid agitated vessels, Can. Journal of Chemical Engineering, 76, 446–455.

Scargiali F., Busciglio A., Grisafi F., Brucato A., 2010a, Simplified Dynamic Pressure Method for k_La measurement in aerated bioreactors, Biochemical Engineering Journal, 49, 165-172.

Scargiali F., Busciglio A., Grisafi F., Brucato A., 2010b, k_La measurement in bioreactors, Chemical Engineering Transactions, 20, 229-234, DOI:10.3303/CET1020039.

Van't Riet K., 1979, Reviewing of measuring method and results in nonviscous gas–liquid mass transfer in stirred vessels, Ind. Eng. Chem. Proc. Des. Dev., 18, 357–364.

Middleton J.C., 1985, Gas-liquid dispersion and mixing. In: Mixing in the Process Industries, Eds. Harnby N., Edward M.F., Nienow A.W., Butterworth, Heidelberg, Germany, 322-355.

Nienow A.W., Langheinrich C., Stevenson N.C., Emery A.N., Clayton T.M., Slater N.K.H., 1996, Homogenisation and oxygen transfer rates in large agitated and sparged animal cell bioreactors: Some applications for growth and production, Cytotecnology, 22, 87-94.

Barrett A.T., Wu A., Zhang H., Levy M.S., Lye G.J., 2010, Microwell engineering characterization for mammalian cell culture process development, Biotechnology and Bioengineering, 105, 260-275.

Linek V., Vacek P., Benes P., 1987, A critical review and experimental verification of the correct use of the dynamic method for the determination of oxygen transfer in aerated agitated vessels to water, electrolyte solutions and viscous liquids, Chem. Eng. J., 34, 11–34.